Efficient Separation of Levulinic Acid Using Fly Ash from Sugar Beet Processing

H. Zeidan and M. E. Marti*
Department of Chemical Engineering,
Konya Technical University,
Konya, Turkey

doi: https://doi.org/10.15255/CABEQ.2024.2292
Original scientific paper
Received: February 13, 2024
Accepted: July 25, 2024

Levulinic acid (LA) is a significant building block in industry. It can be produced by the hydrolysis of lignocellulosic feedstocks and needs to be separated from the aqueous production medium. This study focuses on evaluating fly ash, a waste byproduct from a sugar factory, for use in the adsorption of LA from aqueous media. The sugar beet processing fly ash (SBFA) was characterized using XRD, FTIR, SEM, and N_2 adsorption-desorption analysis. The data fit the pseudo-second-order kinetic model, with good agreement between the experimentally measured (454.55 mg g^{-1}) and calculated (452.40 mg g^{-1}) adsorption capacities. It was observed that the efficiency slightly decreased with increasing temperature, with the effect more pronounced at lower concentrations. Calculated thermodynamic parameters demonstrated that the process was exergonic and exothermic. The capacity of LA adsorption reduced with SBFA dose while enhanced with acid concentration, achieving a maximum of 464 mg LA/g SBFA, higher than values previously achieved with other adsorbents. The Langmuir isotherm model fit well with equilibrium data. Complete recovery of LA was achieved using 0.2 M NaOH, and SBFA could be reused with high efficiency for five consecutive cycles.

Keywords
adsorption, isotherm, levulinic acid, sugar beet fly ash, desorption, reusability

Introduction

The National Renewable Energy Laboratory of the US Department of Energy identifies levulinic acid (LA) as one of the most important compounds derived from biomass that can be used as building blocks for key bio-based chemicals and fuels. Its global market size was USD 83.0 million at the end of 2023, and is projected to grow at a compound annual growth rate (CAGR) of 8.2 % through 2030.[1,2] Levulinic acid has the chemical formula $CH_3C(O)CH_2CH_2CO_2H$, and its keto-acid structure facilitates the synthesis of value-added LA derivatives.[3] The hydrolysis of lignocellulosic materials results in the formation of pentose(s) and hexose(s), which are converted to LA via an acid-catalyzed reaction.[4] Together with its derivatives, LA can be used to produce high-value compounds and biofuels. It has a wide range of applications in many industries, including resin, textiles, plasticizers, antifreeze, animal feed, and paint.[5] However, industry requires high-purity LA for these applications, necessitating its isolation from the production or treatment media.

Many techniques have been tested for the recovery of carboxylic acids from aqueous-based solutions, including fermentation media, effluent, and by-product streams.[6–8] Adsorption is regarded as a promising and effective physicochemical process, particularly for the recovery and removal of compounds, especially from dilute solutions. It offers various advantages, such as cost-effectiveness, simplicity of operation, high adsorption capacity, a sludge-free process, reusability of adsorbents, low energy consumption, high removal efficiency, and selectivity, making it an attractive alternative.[7,9] Industrially produced ion exchange resins have been proposed for this purpose.[10] However, low-cost alternatives need to be explored due to the high cost and regeneration problems associated with resins.[9,11]

Fly ash is an industrial waste by-product that requires proper handling and processing. It may contaminate soil and water, cause respiratory issues, and disrupt biological cycles. The sugar manufacturing process generates large quantities of this substance. Its value-added application is of great interest because its management poses a serious, challenging, and costly environmental concern. Fly ash is typically used as a filler in the manufacture of cements and composite products.[12,13] Reports have also demonstrated its ability to remove or recover compounds from aqueous media.[14–17] However, stud-

*Corresponding author:
Prof. Dr. Mustafa Esen Marti; e-mail: memarti@ktun.edu.tr;
Phone: +90-332-223-1837 Fax: +90-332-241-0635

ies evaluating fly ash for carboxylic acid removal are limited. There are few studies evaluating the effectiveness of fly ash in the adsorption of carboxylic acids.[11,18–20] Kennan and Xavier used a fly ash-activated carbon mixture to separate acetic acid from the medium, though the high cost of activated carbon is a significant disadvantage.[18] Nawle and Patil evaluated fly ash obtained from flue gases in an electrostatic precipitator during coal combustion for acetic acid separation.[19] Soni *et al.* used bagasse fly ash to remove glycolic acid from aqueous solutions.[20] In our previous study, we achieved maximum adsorption capacities of 322 and 336 mg g^{-1} for formic acid and acetic acid using fly ash, respectively.[9]

In this study, fly ash from a sugar beet factory (SBFA) was used as the adsorbent during the adsorptive separation of LA from aqueous solutions. Previous reports have shown that the type of process used to obtain fly ash is critical for the performance of the waste material, as its ingredients and properties change significantly depending on the source and process conditions. Fly ash has often been used for the removal of toxic chemicals such as dyes, metals, and organics from aqueous-based media. However, in this study, we used this waste material as an adsorbent to recover LA, a value-added platform chemical used in the production of unique components and green fuels. We also tested the desorption of the target product, which has not been tested before. Finally, to make the separation economical, we tested the reusability of SBFA in the adsorption process. All these factors make this work novel and valuable for the literature. The adsorbent was characterized using several methods. The recovery of a platform chemical like LA using low-value fly ash has significant potential to reduce the cost of the production method. Capacity values were compared with previously reported results. Isotherms, kinetics, and thermodynamic analyses were conducted, and the effects of process parameters were tested.

Materials and methods

Materials

The fly ash used as adsorbent for separating LA from aqueous solutions was obtained from a sucrose (sugar) plant in Konya, Turkey. The material was used without treatment except for sieving (<53 mesh). It was abbreviated as SBFA since it was obtained from sugar beet processing. The characteristic properties of the studied adsorbent have been previously described.[11] Levulinic acid (LA, 100 % purity) was supplied by Merck Co. Ultra-high pure (UHP) water, produced using the Merck Millipore Direct-Q 3V System, was utilized in all the experiments.

Characterization

The crystal structure of SBFA was analyzed through X-ray diffraction (XRD) using a Bruker D8 Advance X-ray diffraction device with nickel-filtered Cu Kα radiation (Germany) at a voltage of 30 kV and current of 30 mA in a 2θ angular range of 10−90°. Functional group characterization of SBFA was performed using a Fourier transform infrared spectrometer (FTIR; Bruker Vertex 70, Kassel, Germany) with samples prepared by KBr pellets in the range of 400–4000 cm^{-1}. The surface morphology was investigated using Scanning Electron Microscopy (SEM; Zeiss EVO/LS10, Carl Zeiss AG Co., Germany). The specific surface area, pore volume, and average pore diameter of SBFA were determined through Brunauer–Emmett–Teller (BET) and Barrett–Joyner–Halenda (BJH) methods using a TriStar II-3020 Instrument (Micromeritics, USA) with N_2 physisorption at 77 K.

The point of zero charge (pH_{pzc}) of SBFA, which is the pH value at which the overall electric charge of its surface is neutral, was determined. To do this, 45 mL of 0.01 M $NaNO_3$ was added to 100-mL beakers. The initial pH values (pH_i) were adjusted between 2 and 11 by adding HCl or NaOH. Then, 0.1 g SBFA was added, and the final volume was adjusted to 50 mL of 0.01 M $NaNO_3$. The beakers were sealed, and the suspensions were stirred using a magnetic stirrer at room temperature for 12 h, after which the final pH (pH_f) values of the supernatant liquids were measured. The pH_{pzc} of SBFA was determined from the plot of the differences between pH_f and pH_i against initial pH values. The pH_{pzc} of the adsorbent corresponds to the point where the resulting curve intersects the x-axis.

Assay

The initial and residual amounts of LA in the aqueous phase were determined through HPLC analysis using an Agilent LC 1220 instrument. The system included an isocratic pump and a UV detector. Analyses were performed using a C_{18} column (ACE) at 30 °C. The solution of 0.05 mol L^{-1} KH_2PO_4, including 1 % C_2H_3N, at pH 2.8 was utilized as the mobile phase. The flow was set to 1.25 mL min^{-1}.[21] Experiments and analyses were conducted twice, with relative uncertainties of these being less than 1 %.

Equilibrium

Aqueous solutions containing 0.05 to 1.00 M of LA were used in the adsorption experiments. The solutions were prepared using UHP water obtained from a Millipore Direct-Q 3V UHP Water System. The SBFA dose was varied between 0.05–0.50 g/10 mL.

Ten milliliters of LA solutions were mixed with predetermined amounts of SBFA in a 50-mL Erlenmeyer flask, and the phases were shaken at 150 rpm for 60 min. The mixture was centrifuged at 4000 *g* for 2 min to separate the phases upon reaching equilibrium. After carefully removing the supernatant from the system, the amount of residual LA in the aqueous phase was determined. Both the adsorption capacity (q_e) and efficiency (E/%) were calculated using Equations 1 and 2, respectively.

$$q_e = \frac{c_0 - c_e}{m} \cdot V_S \tag{1}$$

$$E(\%) = \frac{c_0 - c_e}{c_0} \cdot 100 \tag{2}$$

Kinetics

Experimental studies were conducted to determine the time needed to achieve the equilibrium, and to monitor the impact of the contact period. The operating conditions were set as follows: SBFA dose of 20 g L^{-1}, LA concentration of 0.25 M, and solution volume of 10 mL. The kinetic experiments were performed over a period of 180 min. The LA concentration in the resulting aqueous portion was then analyzed. Kinetic data were analyzed using four kinetic models: pseudo-first-order (PFO), pseudo-second-order (PSO), Elovich, and intraparticle diffusion (ID) kinetic models. The equations for these models are shown as follows (Eqs. 3–6):[22–25]

$$\text{PFO}\quad \mathrm{d}q_t/\mathrm{d}q = k_1 \cdot (q_e - q_t) \tag{3}$$

$$\text{PSO}\quad \mathrm{d}q_t/\mathrm{d}t = k_2 \cdot (q_e - q_t)^2 \tag{4}$$

$$\text{Elovich}\quad \mathrm{d}q_t/\mathrm{d}t = \alpha \cdot \exp(-\beta \cdot q_t) \tag{5}$$

$$\text{ID}\quad q_t = k_{id} \cdot t^{1/2} + I \tag{6}$$

Thermodynamics

The thermodynamic analysis of the process was conducted by performing experiments at three different temperatures (298–318 K). The initial LA concentration ranged from 0.05 to 1.00 M, with a contact time of 60 minutes. The final concentration of the aqueous phases was determined by HPLC. The data were used to calculate the thermodynamic parameters, including Gibbs free energy ($\Delta G°$), enthalpy ($\Delta H°$), and entropy ($\Delta S°$) changes, using the relevant data and Eqs. 7–9.

$$\Delta G° = \Delta H° - T\Delta S° \tag{7}$$

$$\Delta G° = -R \cdot T \cdot \ln K_L \tag{8}$$

$$\ln K_L = -\frac{\Delta H°}{R \cdot T} + \frac{\Delta S°}{R} \tag{9}$$

Langmuir, Freundlich, and Temkin isotherm models were applied, and the nonlinear expressions of these models are shown in Eqs. 10–13.[26–28]

$$\text{Langmuir}\quad q_e = Q_{max} \cdot \frac{K_L \cdot c_e}{1 + K_L \cdot c_e} \tag{10}$$

$$R_L = 1/(1 + (K_L \cdot c_0)) \tag{11}$$

$$\text{Freundlich}\quad q_e = K_F \cdot [c_e]^{1/n} \tag{12}$$

$$\text{Temkin}\quad q_e = \frac{R \cdot T}{B} \cdot \ln(K_T \cdot c_e) \tag{13}$$

Desorption and reusability

Desorption experiments were conducted using SBFA samples obtained from adsorption, where the initial LA concentration was 0.1 M and the SBFA dose was 0.5 g. For desorption, 0.5 g of LA-SBFA samples were mixed with 10 mL of eluent (0.1 and 0.2 M NaOH) at 150 rpm at 298 K for 60 min. Desorption efficiency (E_D) was calculated using Eq. 14. The regenerated adsorbent was obtained by centrifuging the mixture, followed by washing with distilled water. The regenerated SBFA was then used in successive experiments to assess its reusability.

$$E_D(\%) = \frac{m_{des}}{m_{ads}} \cdot 100 \tag{14}$$

Results and discussion

Characterization

Fig. 1 displays the XRD pattern of SBFA, indicating quartz (SiO_2), mullite ($Al_6Si_2O_{13}$),[29] and some hematite (Fe_2O_3) as the major phases of the sample. The FTIR spectrum in Fig. 2 reveals the asymmetric stretching vibration of Si–O–Si at 1049 cm^{-1} and 781 cm^{-1}, while the peak at 676 cm^{-1} is attributed to the Al–O stretching vibration of $Al_6Si_2O_{13}$.[30,31] The peak at 433.5 cm^{-1} is the characteristic peak of the bending vibrations of Fe–O in Fe_2O_3.[32] These four peaks confirm the presence of mullite, quartz, and hematite, indicating agreement between the FTIR and XRD results. These findings are consistent with previous reports in the literature.[29,33]

Fig. 3 shows the SEM micrographs of SBFA before and after LA adsorption. The SBFA samples exhibited a porous surface and an irregular shape. Variations in the surface morphology of SBFA after adsorption confirmed the presence of LA molecules on the surface. Fig. 4a shows an H3-type hysteresis loop in the type II isotherm, according to the IUPAC classification. This type of isotherm is the most described phenomenon in BET analyses and represents physical adsorption on non-porous or mac-

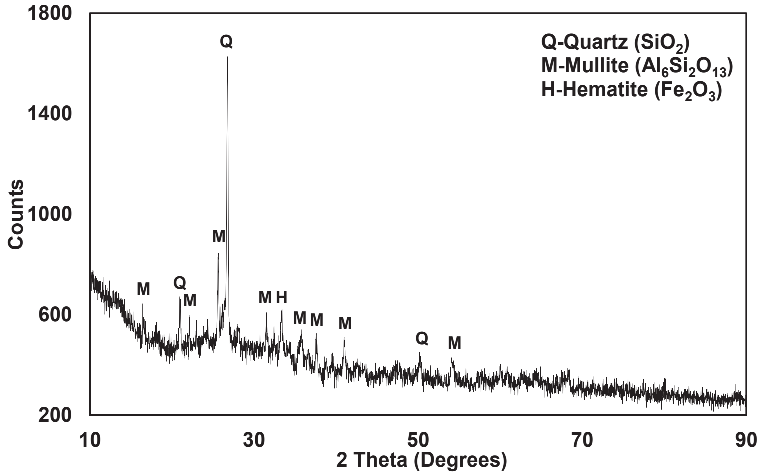

Fig. 1 – *XRD pattern of SBFA*

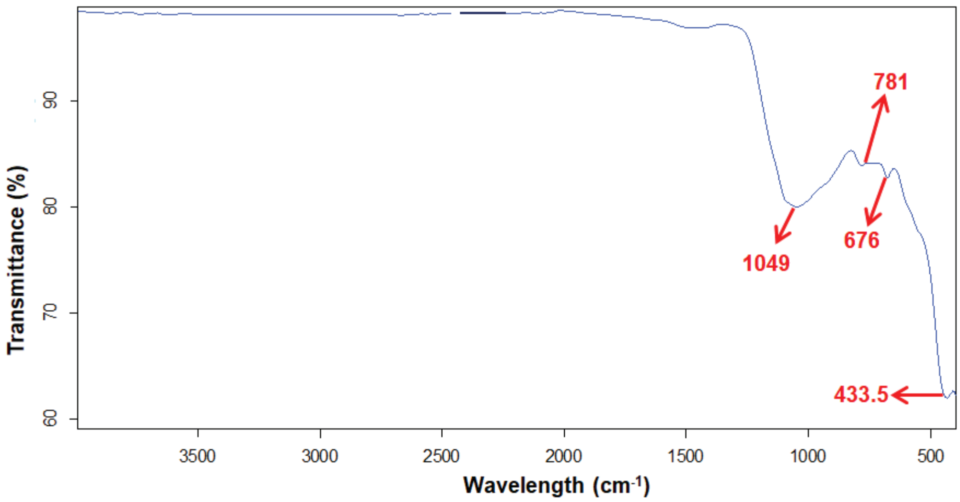

Fig. 2 – *FTIR spectrum of SBFA*

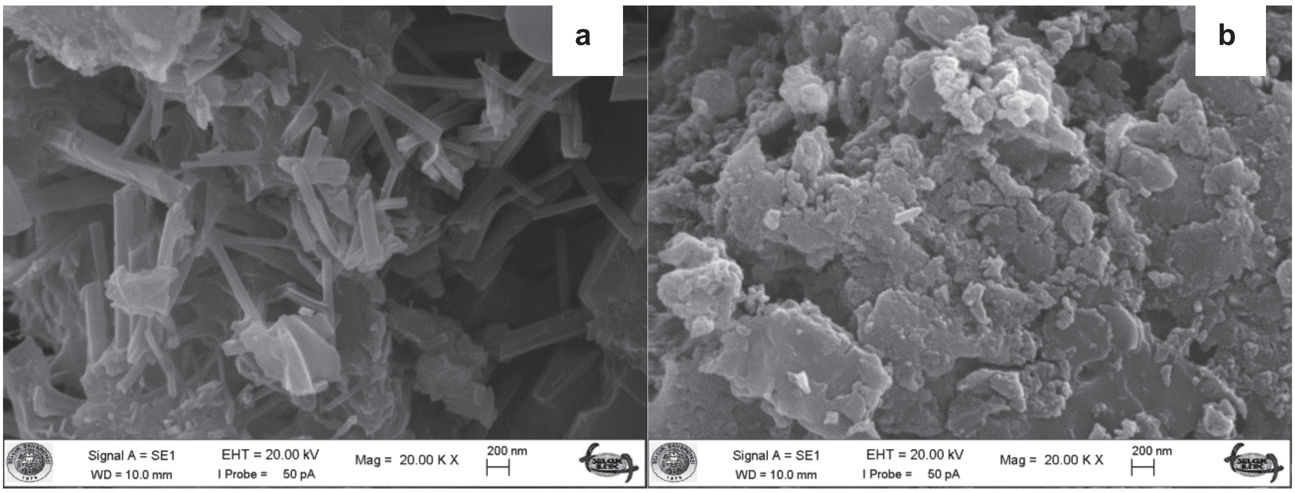

Fig. 3 – *SEM images of a) SBFA, and b) LA loaded-SBFA*

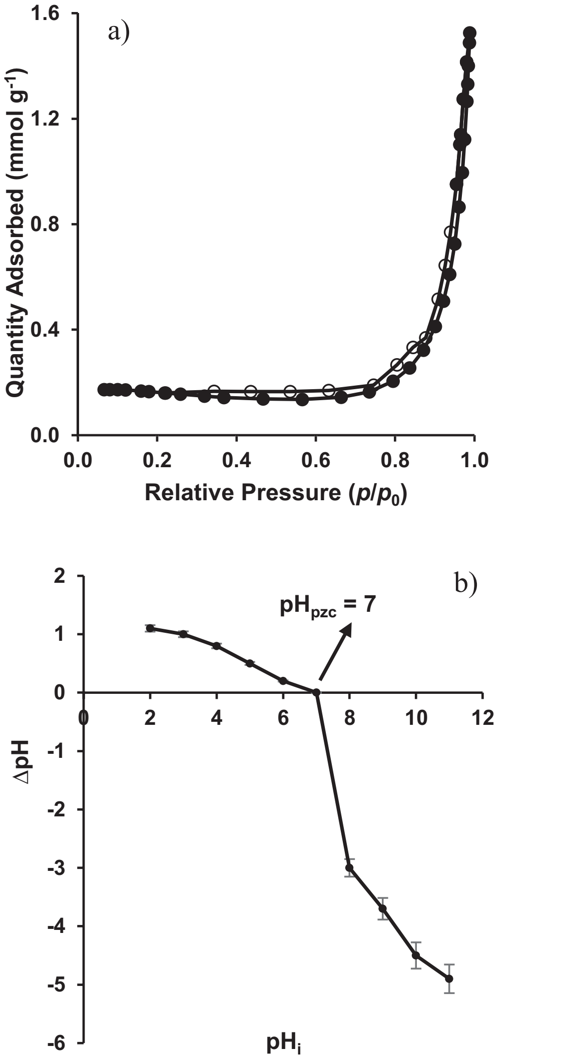

Fig. 4 – *a) Nitrogen adsorption–desorption isotherms at 77 K, b) Point of zero charge of SBFA. Error bars represent standard deviation of uncertainty.*

roporous adsorbents. The specific surface area (S_{BET}), pore volume (V_{BJH}), and average pore diameter (D_{BJH}) of SBFA were calculated to be 15.47 m^2 g^{-1}, 0.0045 cm^3 g^{-1}, and 35.43 nm, respectively. Additionally, the pH_{pzc} of SBFA was calculated, which is the pH value at which the surface charge of the material is equal to zero. According to the data, the pH_{pzc} of SBFA was approximately 7 (Fig. 4b).

Kinetic studies

Adsorption kinetics are essential for estimating the equilibration time, adsorption mechanism, and designing continuous systems.[34] Fig. 5 shows the results from kinetic experiments where the initial LA concentration, SBFA dose, and temperature were constant at 0.25 M, 20 g L^{-1}, and 298 K, respectively. The adsorption rate was rapid over the first 10 min due to the availability of empty surface sites on SBFA for binding LA.[35,36] As these sites became saturated, the adsorption rate slowed down, and reached equilibrium in 60 min. However, the results indicate that separation efficiency is negligibly affected by the contact time between SBFA and LA solution after the first ten minutes (p > 0.05 and f < 5, Table 1). To analyze the data, PFO, PSO, Elovich, and ID models were employed. Model expressions and associated graphs were used to calculate the values of the model constants and determination coefficient (R^2). Fig. 6 and Table 2 show that the R^2 values were 0.9777, ~1.0000 (0.99998), and 0.9608 with PFO, PSO, and Elovich, respectively. Accordingly, the data align well with the PSO kinetic model for the adsorption of LA by SBFA. The experimentally obtained (454.55 mg g^{-1}) and calculated (452.40 mg g^{-1}) adsorption capacities were also in good agreement, indicating that chemisorption controlled the adsorption process.[23,37] The ID model can be used to assess the effect of film and intraparticle diffusion resistance on adsorption.[25,38] The multilinear plot from the ID equation (Fig. 6) indicated three stages: external diffusion, intraparticle diffusion, and equilibrium between adsorbates and adsorbents.[36,39,40] The line did not pass through the origin and multi-linearity was observed, suggesting that other mechanisms may have also controlled the adsorption rate.[41,42]

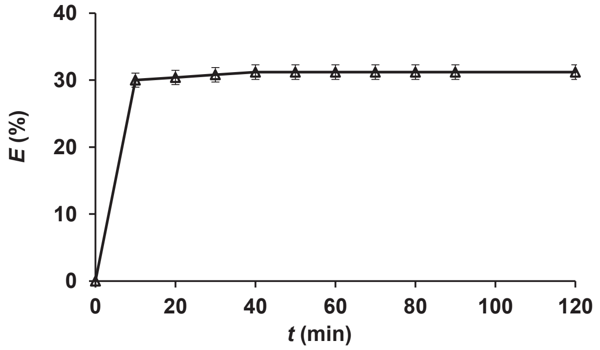

Fig. 5 – *Equilibrium time for the adsorptive separation of LA using SBFA (LA con.: 0.25 M, SBFA dosage: 20 g L^{-1}, temp.: 298 K). Error bars represent standard deviation of uncertainty.*

Table 1 – *Significance of process variables on the separation of LA using SBFA*

Term	p-Value	f-Value
Contact time (min)	0.119	2.97
Temperature (K)	0.744	0.11
Initial acid concentration (M)	$8.40 \cdot 10^{-5}$	21.11
Adsorbent dosage (g L^{-1})	0.005	9.50

* p-value<0.05 & f-value>5: Significant; p-value>0.05 & f-value<5: Insignificant.

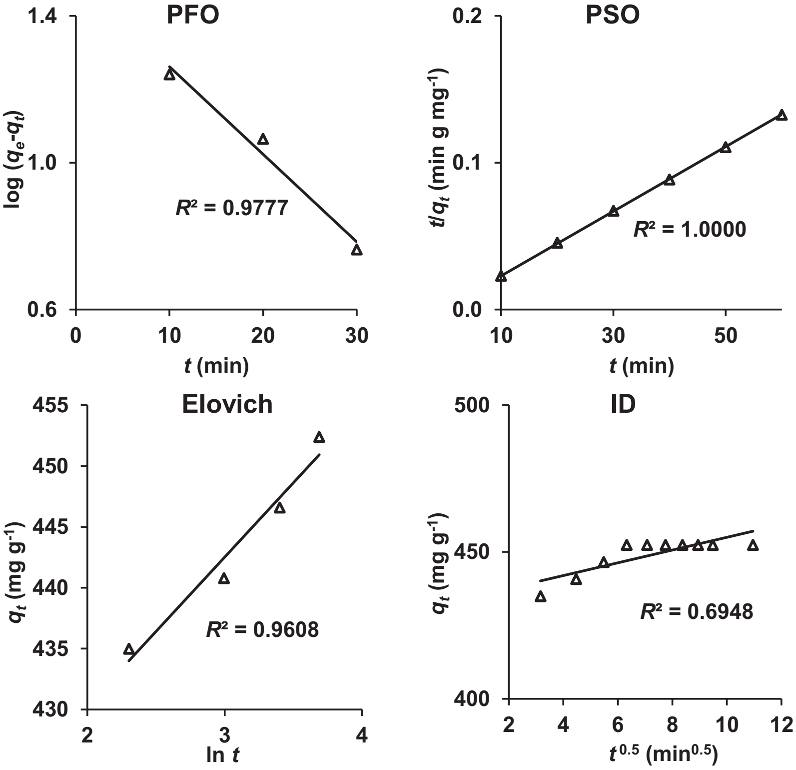

Fig. 6 – *Graphs of the kinetic models for the separation of LA using SBFA (LA con.: 0.25 M, SBFA dosage: 20 g L⁻¹, temp.: 298 K)*

Table 2 – *Constants and determination coefficients of the kinetic models for LA adsorption onto SBFA*

Kinetic models	Constants	
PFO	q_e (mg g^{-1})	31.62 ± 0.45
	k_1 (min^{-1})	0.055 ± 0.001
	R^2	0.9777
PSO	q_e (mg g^{-1})	454.55 ± 2.55
	k_2 (L mol^{-1} min^{-1})	0.0054 ± 0.002
	R^2	1.0000
Elovich	α (mg g^{-1} min^{-1})	$2.246 \cdot 10^{13}$ ± 4.55
	β (g mg^{-1})	12.209 ± 0.55
	R^2	0.9608
ID	k_{id} (mg g^{-1} min$^{-0.5}$)	2.1721 ± 0.02
	I (mg g^{-1})	433.28 ± 3.15
	R^2	0.6948

Thermodynamic studies

Fig. 7 demonstrates the effect of temperature on the recovery of LA from aqueous solutions using SBFA at the values of 298, 308, and 318 K. The adsorbent dose was 20 g L^{-1}, and LA concentrations ranged from 0.05 to 2.0 M. The graph shows that, as temperature increased, both adsorption effectiveness and capacity decreased, though the influence was not significant ($p > 0.05$ and $f < 5$, Table 1). This phenomenon can be attributed to the diminishing cohesive forces between LA molecules and the SBFA surface as the temperature increased.[14] This trend is consistent with many reports in the literature, and indicates the exothermic nature of the process.[11,20] The $\Delta G°$, $\Delta H°$ and $\Delta S°$ values are presented in Table 3. The ($\Delta G°$) values ranged from –7.247 and –8.534 kJ mol^{-1}, suggesting most likely a physical adsorption process. The negative values indicate spontaneous or exergonic nature of LA adsorption. The $\Delta H°$ was found to be –19.548 kJ mol^{-1}, confirming the exothermic nature of the process.[43] The negative value of $\Delta S°$ indicates a decrease in the randomness at the solid-liquid interface during LA adsorption.

Table 3 – *Thermodynamic parameters for the adsorptive separation of LA using SBFA*

T (K)	$\Delta G°$ (kJ mol^{-1})	$\Delta H°$ (kJ mol^{-1})	$\Delta S°$ (J mol^{-1} K^{-1})
298	–8.073 ± 0.12		
308	–8.534 ± 0.14	–19.548 ± 0.25	–37.670 ± 0.45
318	–7.247 ± 0.15		

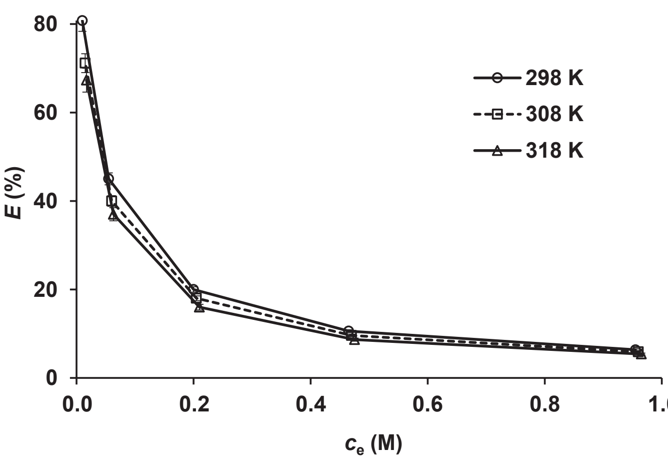

Fig. 7 – *Temperature effect on the adsorptive separation of LA using SBFA (dosage: 20 g L⁻¹). Error bars represent standard deviation of uncertainty.*

Effects of LA concentration and SBFA dose

Fig. 8 shows the isotherm curve for the adsorption of LA by SBFA at a dose level of 30 g L^{-1}. The

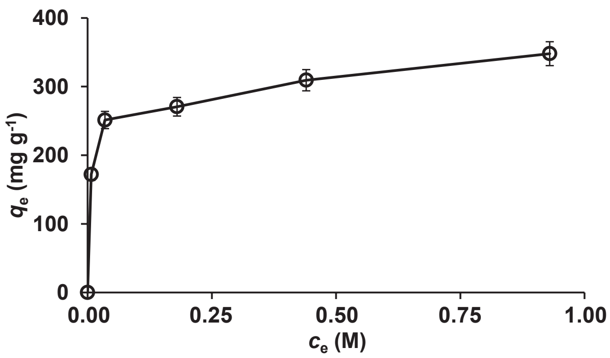

Fig. 8 – *Isotherm curve for the adsorption of LA using SBFA at 298 K and dosage of 30 g L^{-1}. Error bars represent standard deviation of uncertainty.*

data follow Type 1 adsorption characteristics, indicating that the adsorption process can be expressed by the Langmuir isotherm model. The initial SBFA dose and LA concentration ranged from 5 to 50 g L^{-1}, and 0.05 to 1.00 M, respectively. Fig. 9 shows the effects of SBFA dose and LA concentration on efficiency. At a constant SBFA dose, the LA concentration significantly affected adsorption efficiency ($p < 0.05$ and $f > 5$, Table 1), likely due to site saturation on the SBFA surface. Consistent with the literature, adsorption efficiency significantly increased with SBFA dose, as available sites on SBFA increased ($p < 0.05$ and $f > 5$, Table 1).[11,36,38,44] Maximum efficiencies (100 %) were obtained at 0.05 and 0.10 M acid concentration levels and 50 g L^{-1} SBFA. The maximum capacity (q_{max}) reached in this study was 464 mg LA/g SBFA, generally higher than those reported in previous studies using other resins and adsorbents (Table 4).[45–52] This was achieved with an initial dosage of 5 g L^{-1} for SBFA and a LA quantity of 0.05 M. The results support the potential of SBFA to recover carboxylic acids, such as LA, from aqueous-based solutions.

Table 4 – *Maximum adsorption capacities for LA adsorption using different resins and adsorbents in the literature*

Adsorbent	q_{max} (mg g^{-1})	Reference
SBFA	464.00	Present study
SY-01 resin	103.74	45
Amberlite XAD-4	29.04	46
Dry granular activated carbon	142.00	47
D301 resin	185.78	48
D315 resin	147.46	48
Montmorillonite	355.69	49
Cloisite 20A	428.63	49
335 resin	313.50	50
D301 resin	247.31	50
D315 resin	166.04	50
XAD-4 resin	92.00	51
XAD7HP resin	91.00	51
XAD761 resin	136.00	51
Multiwall carbon nanotube (MWCNT)	483.25	52

Adsorption isotherms

Langmuir, Freundlich, and Temkin isotherm models were applied to estimate the binding type of LA onto SBFA.[37,53] The Langmuir model proposes

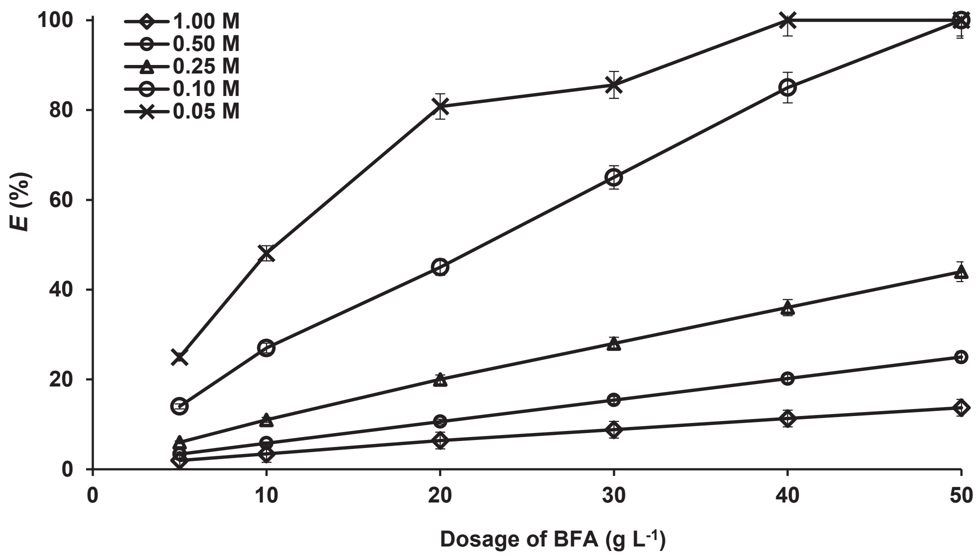

Fig. 9 – *Variation of separation yield with SBFA dose at varied LA amounts. Error bars represent standard deviation of uncertainty.*

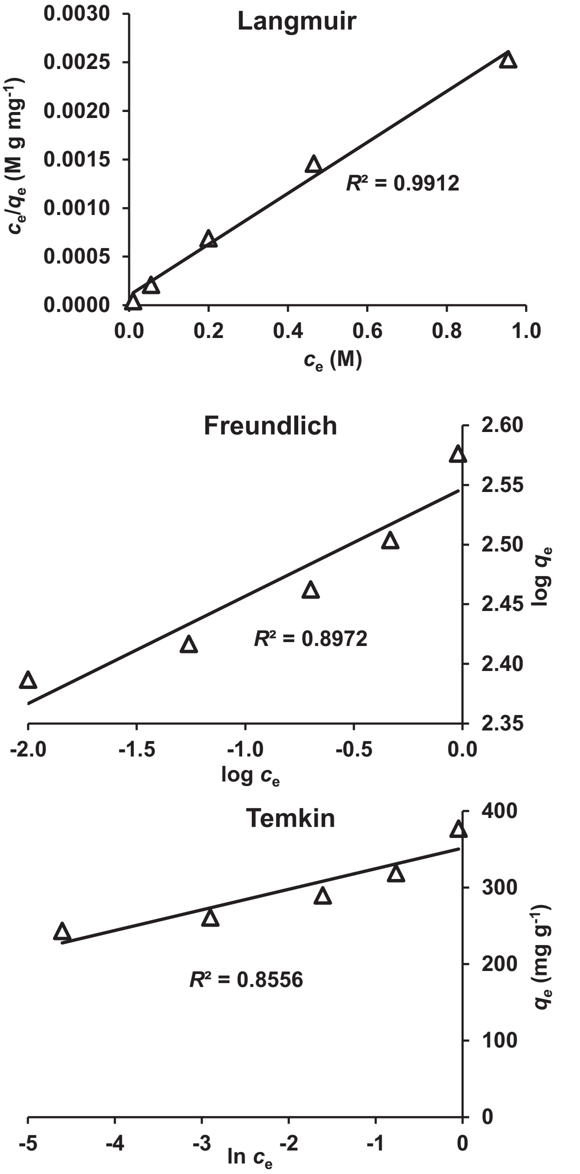

Fig. 10 – *Langmuir, Freundlich, and Temkin isotherms for the adsorption of LA using SBFA at 298 K*

monolayer coverage on a homogenous surface with no interactions between adsorbed molecules. The Langmuir and Freundlich isotherm models explain that adsorption mainly occurs based on chemical and physical forces, respectively. The Freundlich isotherm model also presumes multilayer and non-uniform adsorption on the surface. The Temkin model proposes that the adsorption heat of the adsorbed molecules decreases with surface coverage.[54,55] Non-linear expressions of these models are shown in Eqs. 10–13. Linearized forms of these expressions were used to plot the relevant graphs (Fig. 10). The R^2 values and isotherm model constants are presented in Table 5. The highest R^2 was 0.9912 for the Langmuir isotherm model. A close relationship was observed between the measured (377.00 mg g^{-1}) and estimated (384.61 mg g^{-1}) capacity values, suggesting that the adsorption process is well described by the Langmuir model. Additionally, the process was considered favorable based on the R_L values,[56] indicating good agreement between the Langmuir isotherm model and equilibrium data.

Table 5 – *R^2 values and coefficients for the three isotherm models for the adsorptive separation of LA using SBFA at 298 K*

Isotherm model	Constants	
Langmuir	Q_{max} (mg g^{-1})	384.61 ± 2.33
	K_L (L mg^{-1})	26.00 ± 0.35
	R^2	0.9912
	R_L	(0.010–0.254) ± 0.0001
Freundlich	n	11.11 ± 0.33
	K_f (L mg^{-1})	12.76 ± 0.35
	R^2	0.8972
Temkin	B	26.90 ± 0.44
	K_T (L mg^{-1})	$6.2 \cdot 10^5$ ± 5.00
	R^2	0.8556

Desorption and reusability

Desorption of adsorbate from the adsorbent enables the recovery of the target product, and regeneration of the adsorbent material. Regeneration of the adsorbent is essential to make the process economical and commercially viable. The desorption of LA from SBFA was carried out using NaOH at 0.1 and 0.2 M concentrations. Fig. 11 shows the results. The desorption efficiency was 47 % with 0.1 M NaOH. Increasing the concentration of the desorption agent to 0.2 M resulted in the complete recovery of LA from SBFA.

The reuse of SBFA for LA adsorption was also tested. It was observed that the adsorption efficiency was affected by less than 10 % upon SBFA re-

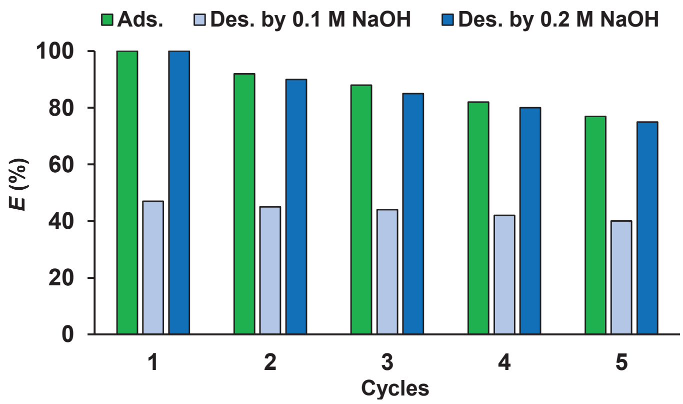

Fig. 11 – *Desorption of LA and reusability of SBFA for the separation of LA from aqueous media (Ads.: $[LA]_o$ = 0.1 M, SBFA dose: 0.5 g, temp.: 298 K, 150 rpm, 60 min; des.: eluent: 0.1 and 0.2 M NaOH, temp.: 298 K, 150 rpm, 60 min)*

use, demonstrating a significant advantage of SBFA. After five cycles, the efficiency of LA adsorption gradually decreased from 100 % to 77 %. Furthermore, the desorption efficiency with 0.2 M NaOH also decreased from 100 % to 75 %.

Conclusions

In this study, sugar beet processing fly ash (SBFA) was evaluated as an adsorbent for the recovery of levulinic acid (LA), a keto-monocarboxylic acid, from aqueous media. The adsorbent was characterized using several techniques. The adsorption system achieved equilibrium after 60 min, and the data aligned well with the pseudo-second-order kinetic model, exhibiting a very high R^2 value. The effect of higher temperatures on the adsorption capacity was minimal, with maximum effectiveness at 298 K. Thermodynamic data indicated that the process was both exothermic and exergonic. The adsorption efficiency increased with the SBFA dose and decreased with the LA concentration, whereas adsorption capacity showed the opposite trend. The maximum capacity was found to be 464.00 mg LA/g SBFA (~4 mmol g^{-1}), significantly higher than the capacities previously reported for several types of resins and adsorbents. The data were in good agreement with the Langmuir isotherm model (R^2 = 0.9912). Desorption of LA was carried out using 0.2 M NaOH, and complete recovery was achieved. SBFA demonstrated high efficiency and reusability for up to five cycles.

FUNDING

The authors acknowledge Konya Technical University for the funding through the Scientific Research Projects Coordination Unit under the Grant Number, 16201046.

NOTES

The authors declare no competing financial interest.

Nomenclature and abbreviations

B – Temkin isotherm constant, J mol^{-1}
c_0 – Initial concentration of levulinic acid, M
c_e – Equilibrium concentration of levulinic acid, M
E – Adsorption efficiency, %
E_D – Desorption efficiency, %
I – Boundary layer diffusion effects (external film resistance), mg g^{-1}
k_1 – Pseudo first order rate constant, min^{-1}
k_2 – Pseudo second order rate constant, L mol^{-1} min^{-1}
k_{id} – Intraparticle diffusion rate constant, mg g^{-1} min$^{-0.5}$
K_F – Freundlich adsorption capacity, L mg^{-1}
K_L – Langmuir equilibrium constant, L mg^{-1}
K_T – Temkin constant, L mg^{-1}
m – Mass of the adsorbent, g
m_{ads} – Mass of adsorbed onto SBFA, g
m_{des} – Mass of LA desorbed from SBFA, g
n – Freundlich heterogeneity constant (adsorption intensity)
q_e – Adsorption capacity at equilibrium, mg g^{-1}
$q_{e(cal)}$ – Calculated adsorption capacity at equilibrium, mg g^{-1}
$q_{e(exp)}$ – Experimental adsorption capacity at equilibrium, mg g^{-1}
q_t – Adsorption capacity at time t, mg g^{-1}
q_{max} – Maximum adsorption capacity, mg g^{-1}
R – Gas constant, 8.314 J mol^{-1} K^{-1}
R_L – Langmuir dimensionless separation factor
R^2 – Determination coefficient
SBFA – Sugar beet processing fly ash
t – Time, min
T – Temperature, K or °C
V – Volume of the aqueous levulinic acid solution, L
α – Elovich initial adsorption rate, mg g^{-1} min^{-1}
β – Elovich desorption constant, g mg^{-1}
$\Delta G°$ – Change in Gibbs free energy, kJ mol^{-1}
$\Delta H°$ – Change in enthalpy, kJ mol^{-1}
$\Delta S°$ – Change in entropy J mol^{-1} K^{-1}

References

1. *Alcocer-García, H., Segovia-Hernández, J. G., Sánchez-Ramírez, E., Caceres-Barrera, C. R., Hernández,* Sequential synthesis methodology in the design and optimization of sustainable distillation sequences for levulinic acid purification, Bioenerg. Res. **17** (2024). doi: https://doi.org/10.1007/s12155-024-10765-0
2. *Jeong, G. T.,* Statistical approach for optimization of levulinic acid production from orange peel as agricultural waste, Biofuel. Bioprod. Biorefin. **17** (2023) 1303. doi: https://doi.org/10.1002/bbb.2498
3. *Girisuta, B., Heeres, H. J.,* Levulinic acid from biomass: Synthesis and applications, in: Fang, Z., Smith, R. L., Qi, X. (Eds.), Production of Platform Chemicals from Sustainable Resources, Biofuel. Biorefin. Springer (2017) 143–169. doi: https://doi.org/10.1007/978-981-10-4172-3_5
4. *Zhang, M., Wang, N., Liu, J., Wang, C., Xu, Y., Ma, L.,* A review on biomass-derived levulinic acid for application in drug synthesis, Crit. Rev. Biotechnol. **42** (2022) 220. doi: https://doi.org/10.1080/07388551.2021.1939261

5. *Ghorpade, V., Hanna, M.,* Industrial applications for levulinic acid. In Cereals: Novel uses and processes Boston, MA: Springer US (1997) 49-55.
doi: https://doi.org/10.1007/978-1-4757-2675-6_7
6. *Uslu, H., Marti, M. E.,* Equilibrium data on the reactive extraction of picric acid from dilute aqueous solutions using Amberlite LA-2 in ketones, J. Chem. Eng. Data **62** (2017) 2132.
doi: https://doi.org//10.1021/acs.jced.7b00226
7. *López-Garzón, C., Straathof, A. J. J.,* Recovery of carboxylic acids produced by fermentation, Biotechnol. Adv. **32** (2014) 873.
doi: https://doi.org/10.1016/j.biotechadv.2014.04.002
8. *Rajendaren, V., Saufi, S. M., Zahari, M. A. K. M.,* A review of the methods for levulinic acid separation and extraction, Biomass Convers. Biorefin. **14** (2022) 1.
doi: https://doi.org/10.1007/s13399-022-03444-7
9. *Zeidan, H., Ozdemir, D., Kose, N., Pehlivan, E., Ahmetli, G., Marti, M. E.,* Separation of formic acid and acetic acid from aqueous solutions using sugar beet processing fly ash: Characterization, kinetics, isotherms and thermodynamics, Desalin. Water Treat. **202** (2020) 283.
doi: https://doi.org/10.5004/dwt.2020.26142
10. *Zeidan, H., Marti, M. E.,* Separation of formic acid from aqueous solutions onto anion exchange resins: Equilibrium, kinetic, and thermodynamic data, J. Chem. Eng. Data **64** (2019) 2718.
doi: https://doi.org/10.1021/acs.jced.9b00128
11. *Asmaly, H. A., Ihsanullah, Abussaud, B., Saleh, T. A., Laoui, T., Gupta, V. K., Atieh, M. A.,* Adsorption of phenol on aluminum oxide impregnated fly ash, Desalin. Water Treat. **57** (2016) 6801.
doi: https://doi.org/10.1080/19443994.2015.1010238
12. *Woszuk, A., Bandura, L., Franus, W.,* Fly ash as low cost and environmentally friendly filler and its effect on the properties of mix asphalt, J. Clean. Prod. **235** (2019) 493.
doi: https://doi.org/10.1016/j.jclepro.2019.06.353
13. *Albaker, R., Kocaman, S., Marti, M. E., Ahmetli, G.,* Application of various carboxylic acids modified walnut shell waste as natural filler for epoxy based composites, J. Appl. Polym. Sci. **138** (2021) 50770.
doi: https://doi.org/10.1002/app.50770
14. *Panday, K. K., Prasad, G., Singh, V. N.,* Copper(II) removal from aqueous solutions by fly ash, Water Res. **19** (1985) 869.
doi: https://doi.org/10.1016/0043-1354(85)90145-9
15. *Akgerman, A., Zardkoohi, M.,* Adsorption of phenolic compounds on fly ash, J. Chem. Eng. Data **41** (1996) 185.
doi: https://doi.org/10.1021/je9502253
16. *Öztürk, N., Kavak, D.,* Adsorption of boron from aqueous solutions using fly ash: Batch and column studies, J. Hazard. Mater. **127** (2005) 81.
doi: https://doi.org/10.1016/j.jhazmat.2005.06.026
17. *Alinnor, I. J.,* Adsorption of heavy metal ions from aqueous solution by fly ash, Fuel **86** (2007) 853.
doi: https://doi.org/10.1016/j.fuel.2006.08.019
18. *Kannan, N., Xavier, A.,* New composite mixed adsorbents for the removal of acetic acid by adsorption from aqueous solutions – a comparative study, Toxicol. Environ. Chem. **79** (2001) 95.
doi: https://doi.org/10.1080/02772240109358979
19. *Nawle, S. C., Patil, S. V.,* Experimental studies on acetic acid removal from waste water using fly ash. In international conference on current trends in technology, Institute of Technology, Nirma University, Ahmedabad **26** (2011) 1.
20. *Soni, A. B., Keshav, A., Verma, V., Suresh, S.,* Removal of glycolic acid from aqueous solution using bagasse fly ash, Int. J. Environ. Res. **6** (2012) 297.
doi: https://doi.org/10.22059/ijer.2011.495
21. *Zeidan, H., Marti, M. E.,* Selective and efficient separation of levulinic, acetic and formic acids from multi-acid solutions by adjusting process parameters, J. Water Process Eng. **56** (2023) 104299.
doi: https://doi.org/10.1016/j.jwpe.2023.104299
22. *Lagergren, S. Y.,* Zur theorie Der Sogenannten adsorption geloster stoffe, Kungliga svenska vetenskapsakademiens **24** (1898) 1.
doi: https://doi.org/10.1007/BF01501332
23. *Ho, Y. S., Mckay, G.,* Pseudo-second-order model for sorption processes, Process Biochem. **34** (1999) 451.
doi: https://doi.org/10.1016/S0032-9592(98)00112-5
24. *Elovich, S. Y., Larinov, O. G.,* Theory of adsorption from solutions of non-electrolytes on solid (I) equation adsorption from solutions and the analysis of its simplest form, (II) verification of the equation of adsorption isotherm from solutions, Izvestiya Akademii Nauk. SSSR, Otdelenie Khimicheskikh Nauk. **2** (1962) 209.
25. *Weber, W. J., Morris, J. C.,* Water Pollution Symposium. Proceedings of 1st International Conference on Water Pollution Research, Pergamon, Oxford **2** (1962) 231–266.
26. *Langmuir, I.,* The constitution and fundamental properties of solids and liquids. Part I. Solids, J. Am. Chem. Soc. **38** (1916) 2221.
doi: https://doi.org/10.1021/ja02268a002
27. *Freundlich, H.,* Über die adsorption in lösungen, Z. Phys. Chem. **57** (1907) 385.
doi: https://doi.org/10.1515/zpch-1907-5723
28. *Temkin, M., Pyzhev, V.,* Kinetics of ammonia synthesis on promoted iron catalysts, Acta Physicochim. URSS **12** (1940) 327.
29. *Kara, S., Aydiner, C., Demirbas, E., Kobya, M., Dizge, N.,* Modeling the effects of adsorbent dose and particle size on the adsorption of reactive textile dyes by fly ash, Desalination **212** (2007) 282.
doi: https://doi.org/10.1016/j.desal.2006.09.022
30. *Kaur, R., Goyal, D.,* Mineralogical comparison of coal fly ash with soil for use in agriculture, J. Mater. Cycles Waste Manag. **18** (2016) 186.
doi: https://doi.org/10.1007/s10163-014-0323-1
31. *Sivalingam, S., Sen, S.,* Optimization of synthesis parameters and characterization of coal fly ash derived microporous zeolite X, Appl. Surf. Sci. **455** (2018) 903.
doi: https://doi.org/10.1016/j.apsusc.2018.05.222
32. *Kalaw, M. E., Culaba, A., Hinode, H., Kurniawan, W., Gallardo, S., Promentilla, M. A.,* Optimizing and characterizing geopolymers from ternary blend of Philippine coal fly ash, coal bottom ash and rice hull ash, Materials **9** (2016) 580.
doi: https://doi.org/10.3390/ma9070580
33. *Wang, N., Xu, H., Li, S.,* A microwave-activated coal fly ash catalyst for the oxidative elimination of organic pollutants in a Fenton-like process, RSC advances **9** (2019) 7747.
doi: https://doi.org/10.1039/c9ra00875f
34. *Zeidan, H., Çufadar, F., Karakaya, N., Karakaya, M. Ç., Marti, M. E.,* Remediation of an aqueous solution contaminated with an anionic diazo dye using natural chabazite, Desal. Water Treat. **317** (2024) 100277.
doi: https://doi.org/10.1016/j.dwt.2024.100277
35. *Banerjee, S., Chattopadhyaya, M. C.,* Adsorption characteristics for the removal of a toxic dye, tartrazine from aqueous solutions by a low cost agricultural by-product, Arab. J. Chem. **10** (2017) 1629.
doi: https://doi.org/10.1016/j.arabjc.2013.06.005

36. *Ali, K., Zeidan, H., Marti, M. E.,* Evaluation of olive pomace for the separation of anionic dyes from aqueous solutions: Kinetic, thermodynamic, and isotherm studies, Desal. Water Treat. **227** (2021) 412.
doi: https://doi.org/10.5004/dwt.2021.27285
37. *Marti, M. E., Zeidan, H.,* Evaluation of beet sugar processing carbonation sludge for the remediation of synthetic dyes from aqueous media, Int. J. Environ. Sci. Technol. **20** (2023) 3875.
doi: https://doi.org/10.1007/s13762-022-04248-y
38. *Zeidan, H., Can, M., Marti, M. E.,* Synthesis, characterization, and use of an amine-functionalized mesoporous silica SBA-15 for the removal of Congo red from aqueous media, Res. Chem. Intermed. **49** (2023) 221.
doi: https://doi.org/10.1007/s11164-022-04876-6
39. *Ozacar, M., Sengil, I. A.,* A two stage batch adsorber design for methylene blue removal to minimize contact time, J. Environ. Manage. **80** (2006) 372.
doi: https://doi.org/10.1016/j.jenvman.2005.10.004
40. *Kooh, M. R. R., Dahri, M. K., Lim, L. B. L., Lim, L. H., Malik, O. A.,* Batch adsorption studies of the removal of methyl violet 2B by soya bean waste: Isotherm, kinetics and artificial neural network modeling, Environ. Earth Sci. **75** (2016) 783.
doi: https://doi.org/10.1007/s12665-016-5582-9
41. *Khaled, A., El Nemr, A., El-Sikaily, A., Abdelwahab, O.,* Treatment of artificial textile dye effluent containing Direct Yellow 12 by orange peel carbon, Desalination **238** (2009) 210.
doi: https://doi.org/10.1016/j.desal.2008.02.014
42. *Tang, C., Shu, Y., Zhang, R., Li, X., Song, J., Li, B., Zhang, Y., Ou, D.,* Comparison of the removal and adsorption mechanisms of cadmium and lead from aqueous solution by activated carbons prepared from *Typha angustifolia* and *Salix matsudana*, RSC Advances **7** (2017) 16092.
doi: https://doi.org/10.1039/C6RA28035H
43. *Altaie, O. T., Zeidan, H., Karakaya, N., Marti, M. E.,* Removal of Congo red from aqueous solutions by adsorption onto illite clay, Desalin. Water Treat. **310** (2023) 226.
doi: https://doi.org/10.5004/dwt.2023.29941
44. *Mall, I. D., Srivastava, V. C., Agarwal, N. K.,* Removal of Orange-G and Methyl Violet dyes by adsorption onto bagasse fly ash—kinetic study and equilibrium isotherm analyses, Dyes Pigm. **69** (2006) 210.
doi: https://doi.org/10.1016/j.dyepig.2005.03.013
45. *Lin, X., Huang, Q., Qi, G., Shi, S., Xiong, L., Huang, C., Chen, X., Li, H., Chen, X.,* Estimation of fixed-bed column parameters and mathematical modeling of breakthrough behaviors for adsorption of levulinic acid from aqueous solution using SY-01 resin, Sep. Purif. Technol. **174** (2017) 222.
doi: https://doi.org/10.1016/j.seppur.2016.10.016
46. *Datta, D., Uslu, H.,* Adsorption of levulinic acid from aqueous solution by Amberlite XAD-4, J. Mol. Liq. **234** (2017) 330.
doi: https://doi.org/10.1016/j.molliq.2017.03.084
47. *Liu, B. J., Liu, S. W., Liu, T. B., Mao, J. W.,* A novel granular activated carbon adsorption method for separation of levulinic acid from formic acid, Adv. Mat. Res. **550–553** (2012) 1691.
doi:
https://doi.org/10.4028/www.scientific.net/AMR.550-553.1691
48. *Liu, B. J., Ren, Q. L.,* Sorption of levulinic acid onto weakly basic anion exchangers: Equilibrium and kinetic studies, J. Colloid Interface Sci. **294** (2006) 281.
doi: https://doi.org/10.1016/j.jcis.2005.07.042
49. *Baylan, N.,* Removal of levulinic acid from aqueous solutions by clay nano-adsorbents: Equilibrium, kinetic, and thermodynamic data, Biomass Convers. Biorefin. **10** (2020) 1291.
doi: https://doi.org/10.1007/s13399-020-00744-8
50. *Liu, B. J., Hu, Z. J., Ren, Q. L.,* Single-component and competitive adsorption of levulinic/formic acids on basic polymeric adsorbents, Colloids Surf. A Physicochem. Eng. Asp. **339** (2009) 185.
doi: https://doi.org/10.1016/j.colsurfa.2009.02.020
51. *Hu, L., Zheng, J., Li, Q., Tao, S., Zheng, X., Zhang, X., Liu, Y., Lin, X.,* Adsorption of 5-hydroxymethylfurfural, levulinic acid, formic acid, and glucose using polymeric resins modified with different functional groups, ACS omega **6** (2021) 16955.
doi: https://doi.org/10.1021/acsomega.1c01894
52. *Çelebican, O., Inci, I., Baylan, N.,* Investigation of adsorption properties of levulinic acid by a nanotechnological material, J. Mol. Struct. **1203** (2020) 127454.
doi: https://doi.org/10.1016/j.molstruc.2019.127454
53. *Musah, M., Azeh, Y., Mathew, J. T., Umar, M. T., Abdulhamid, Z., Muhammad, A. I.,* Adsorption kinetics and isotherm models: A review, CaJOST **4** (2022) 20.
54. *Ragadhita, R. I. S. T. I., Nandiyanto, A. B. D.,* Curcumin adsorption on zinc imidazole framework-8 particles: Isotherm adsorption using Langmuir, Freundlich, Temkin, and Dubinin-Radushkevich models, J. Eng. Sci. Technol. **17** (2022) 1078.
55. *Lu, L., Na, C.,* Gibbsian interpretation of Langmuir, Freundlich and Temkin isotherms for adsorption in solution, Philos. Mag. Lett. **102** (2022) 239.
doi: https://doi.org/10.1080/09500839.2022.2084571
56. *Ali, K., Zeidan, H., Amar, R. B.,* Evaluation of the use of agricultural waste materials as low-cost and eco-friendly sorbents to remove dyes from water: A review, Desalin. Water Treat. **302** (2023) 231.
doi: https://doi.org/10.5004/dwt.2023.29725